

**Fermi National Accelerator Laboratory**

**FERMILAB-Conf-93/120**

# **Chromaticity Compensation Scheme for the Main Injector**

S.A. Bogacz

*Fermi National Accelerator Laboratory  
P.O. Box 500, Batavia, Illinois 60510*

May 1993

Presented at the *1993 Particle Accelerator Conference*, Washington, D.C., May 17-20, 1993

## **Disclaimer**

*This report was prepared as an account of work sponsored by an agency of the United States Government. Neither the United States Government nor any agency thereof, nor any of their employees, makes any warranty, express or implied, or assumes any legal liability or responsibility for the accuracy, completeness, or usefulness of any information, apparatus, product, or process disclosed, or represents that its use would not infringe privately owned rights. Reference herein to any specific commercial product, process, or service by trade name, trademark, manufacturer, or otherwise, does not necessarily constitute or imply its endorsement, recommendation, or favoring by the United States Government or any agency thereof. The views and opinions of authors expressed herein do not necessarily state or reflect those of the United States Government or any agency thereof.*

# Chromaticity Compensation Scheme for the Main Injector

S.A. Bogacz

Accelerator Physics Department, Fermi National Accelerator Laboratory  
P.O. Box 500, Batavia, IL 60510 USA

## Abstract

The current Main Injector lattice is studied in the context of full chromaticity compensation in the presence of the eddy current, saturation and the end-pack sextupole fields generated by the dipole magnets. Two families of correcting sextupole magnets are placed to compensate these fields and to adjust the chromaticity (in both planes) to some desired value. Variation of the dipole induced sextupole fields with the B-field (changing along a ramp) are modeled according to recent experimental measurements of the Main Injector dipole magnet. Analysis of the required sextupole strengths is carried out along two realistic momentum ramps. The results of our calculation give quantitative insight into the requisite performance of the sextupole magnets.

## I. CHROMATICITY COMPENSATION

In addition to the dipoles and quadrupoles the Main Injector lattice includes two families of sextupole magnets (focusing and defocusing) located in the regular cells adjacent to the respective quadrupoles. The integrated strength,  $S$ , of an individual sextupole of length  $L$  (in geometric units of  $m^{-2}$ ) is introduced as a thin element as follows

$$\Delta x' = S x^2 \quad (1)$$

There is also additional sextupole field induced by each dipole magnet. This field combines the effect of eddy current as well as sextupole saturation and the geometric end-field effects. Here, one implements it by inserting a zero-length sextupoles at the middle of each dipole and at both ends (to mock-up the effects of the above fields). The integrated sextupole strengths corresponding to the 'body' and 'ends' effects are defined as follows

$$S_b = \theta_{\text{dip}} (b_2^{\text{edd}} + b_2^{\text{sat}}), \quad (2)$$

$$S_e = \theta_{\text{dip}} b_2^{\text{end}},$$

where  $\theta_{\text{dip}}$  is the bend angle of the dipole magnet.

The goal of these two families of sextupoles (f and d) is to compensate the natural chromaticity,  $\underline{\chi}^0$ , in the presence of the dipole sextupoles,  $S_b$  and  $S_e$ , to some desired value,  $\underline{\chi}$ , (both in the horizontal and vertical planes). One can describe the above compensation scheme in the following convenient notation (in terms of eight sensitivity coefficients)

$$\underline{\chi} = \underline{\chi}^0 + \mathbf{M} \begin{pmatrix} S_f \\ S_d \end{pmatrix} + \mathbf{S} \begin{pmatrix} S_b \\ S_e \end{pmatrix} \quad (3)$$

Here, the underlined symbols denote 2-dim column vectors and the bold face characters represent two-by-two matrices. These two dimensional objects correspond to the horizontal and vertical degrees of freedom. One can easily identify the eight sensitivity coefficients with the components of  $\mathbf{M}$  and  $\mathbf{S}$  matrices.

It is useful to express the sextupole strength in magnetic units of Tesla/m. Therefore, one introduces a column vector strength,  $\underline{g}$ . Its components describe the sextupole strength of both families as follows

$$\underline{g} = (B_0 \rho) \begin{pmatrix} S_f \\ S_d \end{pmatrix} \quad (4)$$

where  $\rho$  is a local curvature radius. Solving Eq.(3) with respect to  $\underline{g}$  and applying Eqs.(2), yields the following formula

$$\underline{g} = (B_0 \rho) \mathbf{M}^{-1} [\underline{\chi} - \underline{\chi}^0 - \mathbf{S} \begin{pmatrix} S_b \\ S_e \end{pmatrix}] \quad (5)$$

The above expression is used to analyze the required sextupole strength as a function of changing B-field along two basic Main Injector ramps for different chromaticity compensations. The sensitivity coefficients for three families of sextupoles,  $\mathbf{S}$  and  $\mathbf{M}$ , are simulated for the Main Injector lattice using MAD tracking code<sup>1</sup>. The resulting coefficients along with the natural chromaticity,  $\underline{\chi}^0$ , are listed below

$$\mathbf{M} = \begin{pmatrix} 8.28 & 0.901 \\ -1.82 & -4.43 \end{pmatrix} \times 10^2,$$

$$\mathbf{S} = \begin{pmatrix} 1.49 & 3.50 \\ -1.39 & -3.00 \end{pmatrix} \times 10^3, \quad (6)$$

$$\underline{\chi}^0 = \begin{pmatrix} -33.6 \\ -32.9 \end{pmatrix}.$$

To complete the sextupole strength analysis, outlined by Eq.(5), one has to gain some insight into the sextupole content of a dipole magnet and its variation with B-field.

## II. SEXTUPOLE CONTENT OF A DIPOLE MAGNET

First, we consider the sextupole field induced by the eddy current flowing in the dipole magnet lamination. Assuming that the field is proportional to the eddy current density, which in turn is linear in  $\dot{B}_0$ , one gets immediately the following relationship

$$b_2^{\text{edd}} = 8.128 \times 10^{-2} \frac{\dot{B}_0}{B_0} \quad [\text{m}^{-2}], \quad (7)$$

Here, the numerical proportionality coefficient was found<sup>2</sup> through numerical simulations.

Combined contribution of the saturation and static sextupole fields was found experimentally<sup>3</sup> via the flat and rotating coil measurements of the dipole magnet. The resulting sextupole strength variation with B-field is illustrated in Figure 1.

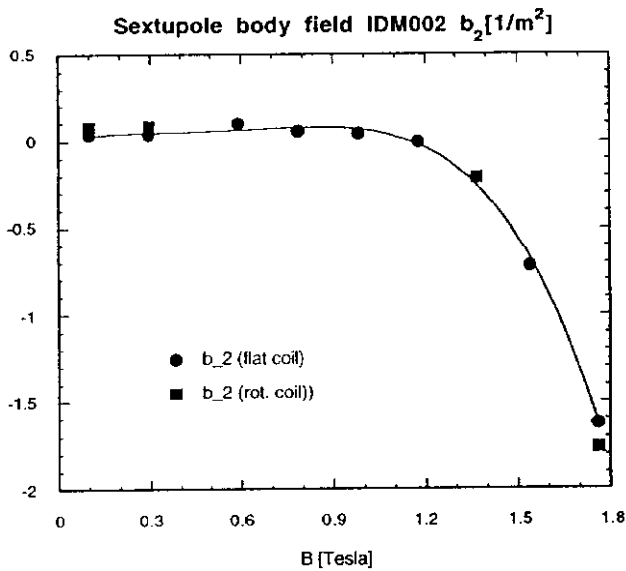


Figure 1

Finally, the end-field effect was measured for various geometries of the end-pack piece. They are collected in Figure 2. The end-pack #9 was selected as the design configuration for the dipole magnet end-pack.

Further analysis of the sextupole strength will be carried out for two realistic Main Injector ramps<sup>4</sup>, namely the 150 GeV 'standard ramp' and the 120 GeV 'slow spill ramp'. To summarize the dipole content of the sextupole all three contributions are plotted as a function of momentum for 150 GeV 'standard ramp'. Figure 3 illustrates the above plots.

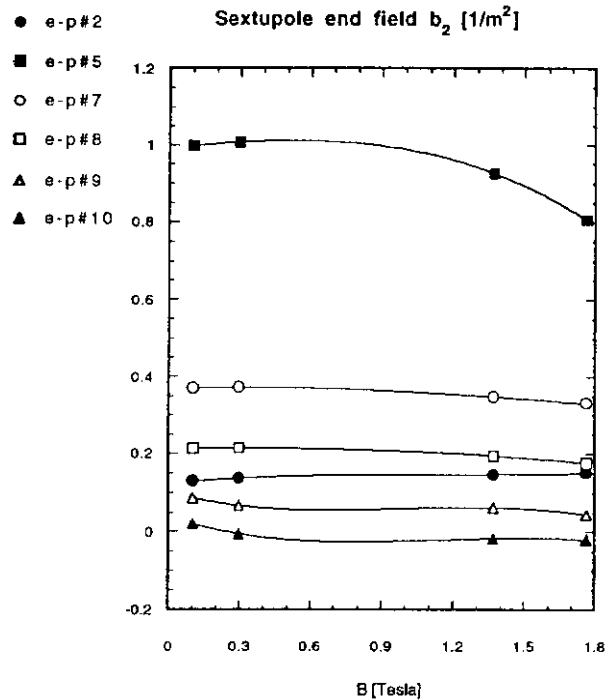


Figure 2

As one may have expected, the dipole sextupole at low B-fields starts at some static plateau and it is virtually dominated by the eddy current sextupole, while at higher B-fields the saturation component picks up and it eventually shapes up the sextupole field profile at the end of a ramp.

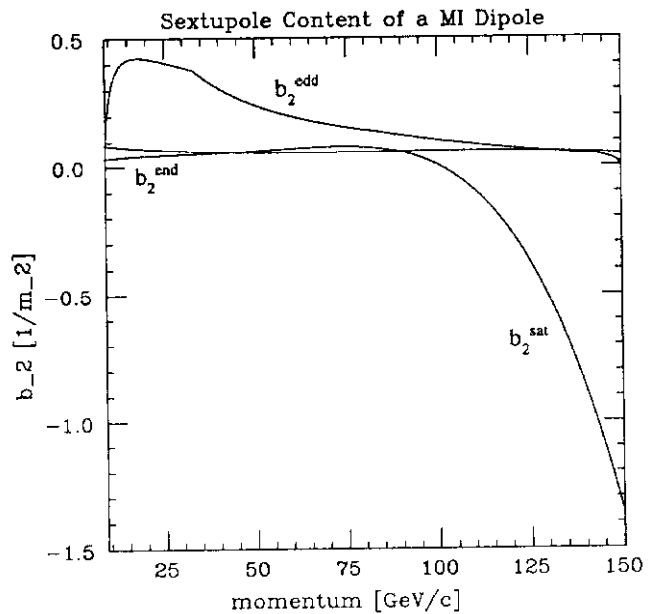


Figure 3

### III. SEXTUPOLE STRENGTH – CONCLUSIONS

Now, one can evaluate the correcting sextupole strength,  $\underline{g}$ , given by Eq.(5), for every point along a given momentum ramp (using values of  $b_2$ 's taken from Figure 3). This procedure will generate the sextupole strength ramps for both families of correcting sextupoles (f and d). Figures 4 and 5 summarize final sextupole requirements for two model ramps. This assumes chromaticity flip at transition (from -10 units before transition to 10 units above transition, linearly, over a 20 msec time interval). The last condition is dictated by the head-tail instability assessment<sup>5</sup> carried out for the Main Injector.

Certain care is taken to maintain unipolarity of the power supplies for both families of correcting sextupoles (appropriate choice of the end-pack geometry). By convention, the focusing family carries positive and the defocusing one negative sign of the integrated sextupole strengths.

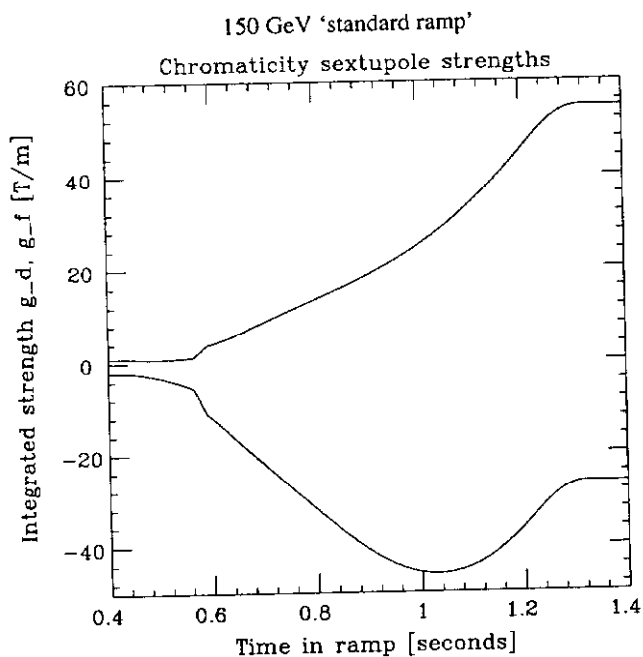


Figure 4

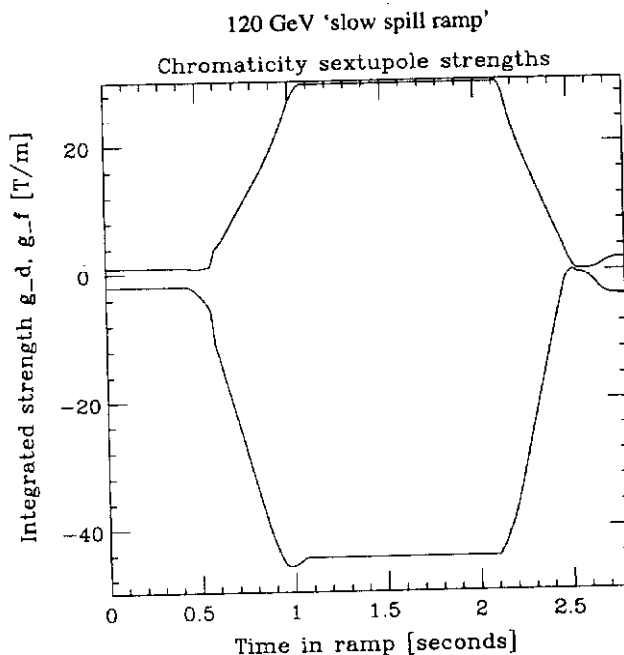


Figure 5

As one can see from Figures 4 and 5, the extreme value of the defocusing sextupole strength is bound by 45 Tesla/m for both ramps, while the maximum required strength of the focusing family in case of the regular 150 GeV ramp (55 Tesla/m) is much higher than the corresponding strength for the slow spill 120 GeV ramp (30 Tesla/m). This last feature is a result of smaller saturation sextupole component in case of the slow spill ramp (see Figure 3). The above extreme values of the sextupole strength for both families translate into the current/voltage requirements for the sextupole magnet design, which sets the standard for their power supplies performance.

#### REFERENCES

1. H. Grote and C. Iselin, The MAD program users reference guide, CERN/SL/90-13 (AP), 1990.
2. J-F. Ostiguy, Eddy current induced multipoles in the Main Injector, FERMILAB MI-0037, 1990.
3. H. Glass, Private Communication.
4. P. Martin, 150 GeV and revised 120 GeV Ramps, FERMILAB MI-0027A, 1990.
5. S.A. Bogacz, Coherent instability limits - Supplement, FERMILAB FN-507, 1989.